**DRAFT**
EIC PDR
October 7, 2024

# Electron Ion Collider

# Preliminary Design Report
# (this report only contains TOF part)

## Contributors:

E-C. Aschenauer[1], R. Ent[2], ADD NAMES AND INSTITUTIONS

[1]Brookhaven National Laboratory, USA
[2]Thomas Jefferson National Accelerator Facility, USA

# Contents

# List of Figures

# List of Tables

multi-chapters

# Chapter 8

# Experimental Systems

## 8.1 Experimental Equipment Requirements Summary

Add text here.

## 8.2 General Detector Considerations and Operations Challenges

### 8.2.1 General Design Considerations

Add text here.

### 8.2.2 Backgrounds and Rates

Add text here.

### 8.2.3 Radiation Level

Add text here.

## 8.3 The ePIC Detector

### 8.3.1 Introduction

Hello, here is some text without a meaning [1].


**Figure 8.1:** Test Figure.

### 8.3.2 Magnet

**Requirements**

**Requirements from physics:** Add text here.

**Requirements from Radiation Hardness:** Add text here.

**Requirements from Data Rates:** Add text here.

**Justification**

**Device concept and technological choice:** Add text here.

**Subsystem description:**

General device description: Add text here.

Sensors: Add text here.

FEE: Add text here.

Other components: Add text here.

**Requirements from Data Rates:** Add text here.

**Implementation**

**Services:** Add text here.

**Subsystem mechanics and integration:** Add text here.

**Calibration, alignment and monitoring:** Add text here.

**Status and remaining design effort:**

R&D effort: Add text here.

E&D status and outlook: Add text here.

Other activity needed for the design completion: Add text here.

Status of maturity of the subsystem: Add text here.

**Environmental, Safety and Health (ES&H) aspects and Quality Assessment (QA planning:** Add text here.

**Construction and assembly planning:** Add text here.

**Collaborators and their role, resources and workforce:** Add text here.

**Risks and mitigation strategy:** Add text here.

**Additional Material** Add text here.

### 8.3.3 Tracking

Add text here.

#### 8.3.3.1 The silicon trackers

**Requirements**

**Requirements from physics:** Add text here.

**Requirements from Radiation Hardness:** Add text here.

**Requirements from Data Rates:** Add text here.

**Justification**

**Device concept and technological choice:** Add text here.

**Subsystem description:**

General device description: Add text here.

Sensors: Add text here.

FEE: Add text here.

Other components: Add text here.

**Performance**

**Implementation**

**Services:** Add text here.

**Subsystem mechanics and integration:** Add text here.

**Calibration, alignment and monitoring:** Add text here.

**Status and remaining design effort:**

R&D effort: Add text here.

E&D status and outlook: Add text here.

Other activity needed for the design completion: Add text here.

Status of maturity of the subsystem: Add text here.

**Environmental, Safety and Health (ES&H) aspects and Quality Assessment (QA planning:** Add text here.

**Construction and assembly planning:** Add text here.

**Collaborators and their role, resources and workforce:** Add text here.

**Risks and mitigation strategy:** Add text here.

**Additional Material** Add text here.

#### 8.3.3.2 The MPGD trackers

**Requirements**

**Requirements from physics:** Add text here.

**Requirements from Radiation Hardness:** Add text here.

**Requirements from Data Rates:** Add text here.

**Justification**

**Device concept and technological choice:** Add text here.

**Subsystem description:**

General device description: Add text here.

Sensors: Add text here.

FEE: Add text here.

Other components: Add text here.

**Performance**

**Implementation**

**Services:** Add text here.

**Subsystem mechanics and integration:** Add text here.

**Calibration, alignment and monitoring:** Add text here.

**Status and remaining design effort:**

R&D effort: Add text here.

E&D status and outlook: Add text here.

Other activity needed for the design completion: Add text here.

Status of maturity of the subsystem: Add text here.

**Environmental, Safety and Health (ES&H) aspects and Quality Assessment (QA planning:** Add text here.

**Construction and assembly planning:** Add text here.

**Collaborators and their role, resources and workforce:** Add text here.

**Risks and mitigation strategy:** Add text here.

**Additional Material** Add text here.

### 8.3.4 Particle identification

Add text here.

#### 8.3.4.1 The time-of-flight layers

**Requirements and Justifications**

**Requirements from physics:** With single hit timing resolution of 35 ps from the Barrel TOF (BTOF) and 25 ps from the Forward TOF (FTOF), the AC-LGAD TOF detector system can provide particle identification for low momentum charged particles, e.g., $\pi$-$K$ separation at the $3\sigma$ level for $p_T < 1.2$ GeV/c for $-1.2 < \eta < 1.6$, and $p < 2.5$ GeV/c for $1.9 < \eta < 3.6$, respectively. By combining the PID information for low momentum particles from the TOF detectors and high momentum particles from Cherenkov detectors, ePIC will have excellent PID capability over a wide momentum range in a nearly $4\pi$ acceptance, which is crucial to achieve the goals of the EIC physics program. Besides precise timing resolution, AC-LGAD sensors can also provide precise spatial resolution, and thus aid track reconstruction and momentum determination. The requirements on the timing and spatial resolutions, as well as the material budgets are being evaluated in ePIC MC simulation to find the optimal configuration without over-designing these detectors. Table 8.1 summarizes the current specifications of the timing and spatial resolutions, material budgets, the covered area,

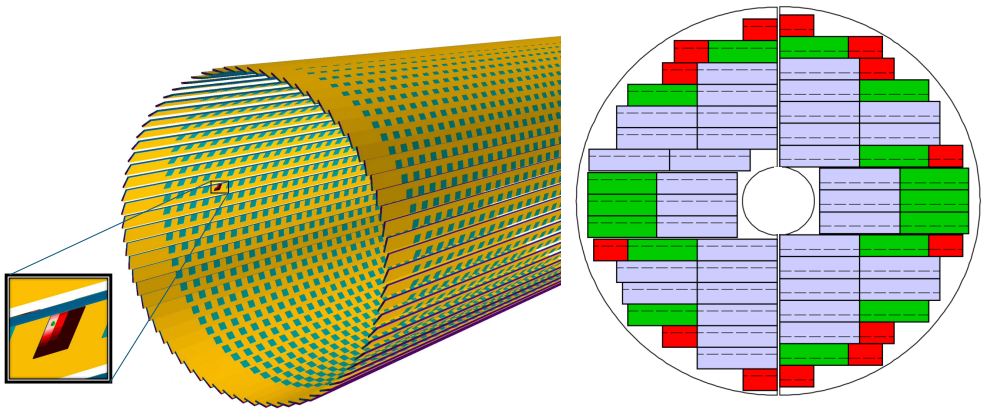

**Figure 8.2:** Geometries of BTOF with insert of sensor and charge sharing distribution (left), and the layout of sensor modules and service hybrids of FTOF on one side (right).

channel counts and dimensions. Figure 8.2 shows the BTOF and FTOF layouts with an insert showing charge sharing on a sensor. Figure 8.3 shows the performance of the TOF detector in the form of $1/\beta$ as a function of particle momentum $p$ for $ep$ DIS events from PYTHIA+GEANT4 simulation. Together with the other PID detectors, we are able to demonstrate that the ePIC PID performance which includes the TOF detectors as one of the integral components meets the requirements.

| **Subsystem** | Area ($m^2$) | dimension ($mm^2$) | channel count | timing $\sigma_t$ (ps) | spatial $\sigma_x$ ($\mu$m) | material budget ($X_0$) |
|---|---|---|---|---|---|---|
| Barrel TOF | 12 | 0.5*10 | 2.4M | 35 | 30 ($r \cdot \phi$) | 0.015 |
| Forward TOF | 1.1 | 0.5*0.5 | 3.2M | 25 | 30 ($x, y$) | 0.05 |

**Table 8.1:** Required performance for physics and proposed configurations for the TOF detector system.

**Requirements from Radiation Hardness:** The radiation fluence and dose at ePIC are significantly less than in the LHC experiments. It is safe to assume that the maximum foreseen fluence for the lifetime of the TOF detectors will be $< 5 \times 10^{12}$ $n_{eq}/\text{cm}^2$, as seen in Fig. 8.4 and Tab. 8.2. Here the highest fluence between raw and 1MeV $n_{eq}/\text{cm}^2$ fluence was considered, as the standard NIEL correction is not applicable for some aspects of LGAD radiation damage.

Much work has been done to characterize and improve the radiation resistance of LGAD gain layers to meet the requirements at the LHC [2] (up to $2.5 \times 10^{15}$ 1MeV $n_{eq}/\text{cm}^2$). Because of the sensitivity of the sensor performance to the value of the N+ sheet resistance (a feature absent from the conventional LGADs made use of for the LHC), it is possible that AC-LGADs may be significantly less radiation tolerant than their conventional cousins. Indeed, N-type doping is known to be particularly sensitive to hadronic irradiation, with N-bulk sensors inverting to P-bulk before exposure of even $1 \times 10^{14}$ is accumulated. Furthermore, LHC LGAD detectors are designed to run at -30C to reduce the post-radiation leakage current, while in ePIC, the sensors will be operated at room or slightly lower temperatures for the experiment's lifetime. The leakage current increase due to radiation damage for the fluence in ePIC has to be low enough not to trigger a thermal runaway combined with the power dissipation from the readout chip, especially for the forward and

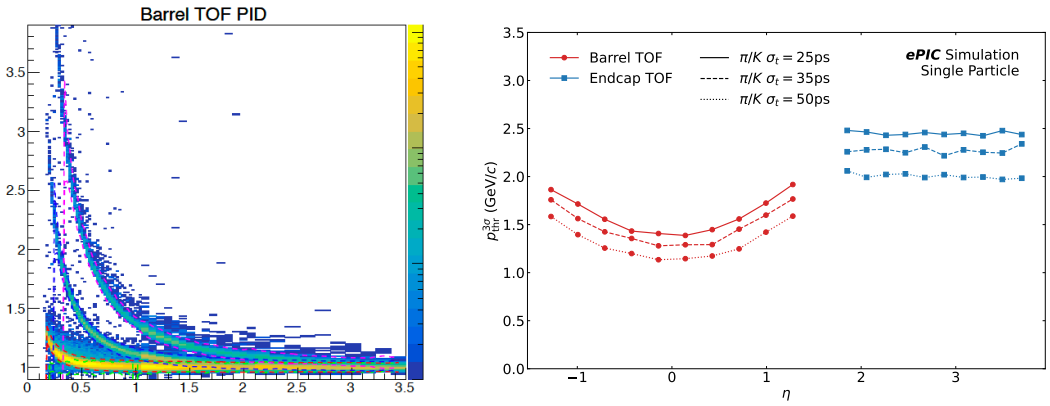


**Figure 8.3:** BTOF $1/\beta$ as a function of momentum (p) in the simulation performance with PYTHIA DIS events (left). Upper limits on the $3\sigma$ particle separation from BTOF and FTOF as a function of pseudorapidity (right).

end-cap region where the chips are bump bonded on top of the sensors.

Therefore, a radiation exposure run was performed before the ePIC LGAD design was finalized. Several sensors from HPK and BNL were irradiated at FNAL ITA facility (400 MeV protons) and at the TRIGA reactor in Ljubljana (MeV-scale neutrons) to probe radiation effect from ionizing and non-ionizing particles. The radiation exposure would be done in steps, allowing potential charge-collection pathologies, should they exist, to be mapped out for the development of models and corrections. By studying the sensor performance before and after irradiation, the change in N+ resistivity can be characterized, and this particular risk can be addressed. Sensors irradiated with 1 MeV neutrons were received in the Summer of 2024 and tested; the results are encouraging, as seen in the following sections. Sensors were irradiated at the FNAL ITA facility but are still cooling down from the activation; they will likely be available for testing in early 2025.

| RAW fluence | | | |
|---|---|---|---|
| System | Average | Min | Max |
| Barrel | $5.4 \times 10^{10}$ | $3.4 \times 10^{10}$ | $5.9 \times 10^{11}$ |
| End-cap | $1.3 \times 10^{11}$ | $5.1 \times 10^{10}$ | $1.6 \times 10^{12}$ |
| B0 trackers | $3.9 \times 10^{11}$ | $3.3 \times 10^{10}$ | $1.8 \times 10^{12}$ |
| NEQ fluence | | | |
| System | Average | Min | Max |
| Barrel | $3.6 \times 10^{10}$ | $1.1 \times 10^{10}$ | $1.3 \times 10^{12}$ |
| End-cap | $1.2 \times 10^{11}$ | $3.2 \times 10^{10}$ | $8.4 \times 10^{11}$ |
| B0 trackers | $4.5 \times 10^{11}$ | $2.7 \times 10^{10}$ | $4.2 \times 10^{12}$ |

**Table 8.2:** RAW and NEQ fluence per system for the lifetime of the ePIC experiment, assuming 10 years of data taking at 50% time.

**Requirements from Data Rates:** As the sensors and ASICs differ between the BTOF and FTOF, the rate requirements are presented separately for both of these sub-components. On top of that,

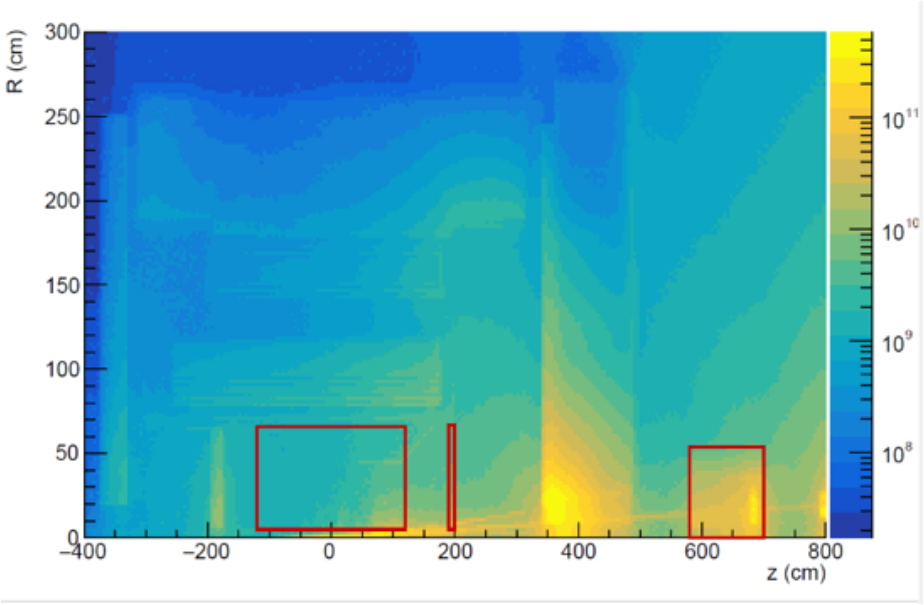


**Figure 8.4:** Fluence accumulated for 6 months at 100% time, corresponding to one year of data taking, the fluence has to be multiplied by the assumed 10 years of life time of the ePIC detector. Red squares highlight the barrel, end-cap, and B0 trackers detectors.

the phase space coverage is different (mid-rapidity vs forward rapidity) which mandates different particle rate and background calculations.

**BTOF:** The BTOF simulations show an average of 5 charged particles per *ep* collision at the highest center of mass energy. At the 500 kHz collision rate this amounts to a 2.5 MHz particle rate on the surface of the BTOF barrel. BTOF contains 2.4 million channels which give an average hit frequency per channel of 1 Hz. Due to charge sharing of the AC-LGAD strips we expect a particle to generate signals on maximum 3 strips/channels of the readout ASIC.

**FTOF:** The FTOF simulation shows an average of 2 charged particles per *ep* collision at the highest center of mass energy. At the 500 kHz collision rate this amounts to a 1 MHz particle rate on the surface of FTOF disk. Since FTOF is expected to contain 5.8 million channels the average hit frequency per channel is 0.2 Hz. Due to charge sharing of the AC-LGAD pixels we expect a particle hit to generate signals on maximum 3x3 pixels/channels of the readout ASIC.

**Electronics Noise:** Noise measurements have consistently shown a rate of 30 Hz per channel. Such a noise rate is achieved with a 5-sigma cut and is deemed to be even somewhat pessimistic but this is the number we plan to use during these calculations.

**Data Rates:** We will assume a typical CERN-developed ASIC's zero-suppressed data format which is: 32 bits header, Nx32 bits of channel data (ADC, TDC, ch Id) and 32 bits trailer. Such data formats are used in e.g. HGCROC which is a precursor to our expected ASICs.

For BTOF the expected signal rate of bits per second per ASIC is 1 Hz (particle rate) x 5 x 32 (bits for 3 hits) X 64 (channels) = 10 kbps, while the noise rate is 30 Hz (noise) x 3 x 32 (bits for a single hit) X 64 (channels) = 185 kbps. Summing up these 2 contributions we reach the total data rate per-ASIC of 195 kbs. Since an RDO reads out 128 ASICs per half stave we expect a rate per RDO (or fiber) of 24 Mbps. For the entire BTOF which contains 288 half staves we reach a total rate requirement of 7

Gbps.

For FTOF the expected signal rate of bits per second per ASIC is 0.2 Hz (particle rate) X 11 x 32 (bits for 9 hits) X 1024 (channels) = 72 kbps, while the noise rate is 30 Hz (noise rate) X 3 x 32 (bits for a single hit) X 1024 (channels) = 3000 kbps. Summing up these 2 contributions we arrive at the per-ASIC data rate of 3.1 Mbps. For the worst case of 28 ASICs per RDO (or fiber) = 87 Mbs per fiber link to DAQ. For the total FTOF sub-detector of 212 RDOs we reach 18 Gbps.

We note that these rates are very small and well within the reach of ASICs, interconnects as well as fiber interfaces of our electronics and DAQ. We also note that the data rates are dominated by the electronics noise which we can control by raising or lowering the various ADC or TDC thresholds of the ASIC thus adjusting the system performance even ASIC-to-ASIC if required.

**Device concept and technological choice:** AC-coupled Low-Gain Avalanche Diode (AC-LGAD) is a new silicon sensor technology. Signals produced by charged particles in the sensor active volume are amplified via an internal p+ gain layer near the sensor surface. Signals induced on a continuous resistive n+ layer on top of the p+ gain layer, are AC coupled to patterned metal readout electrodes, which are on the sensor surface and separated by a dielectric layer from the n+ layer. The internal signal amplification and thin active volume enables precise timing measurement, while charge sharing among neighboring electrodes can provide precise position measurement. The AC-LGAD technology has been chosen to use for particle identification, tracking, and far-forward detectors at EIC where precision timing and spatial measurements are needed.

**Subsystem description:**

**General device description**: The BTOF consists of 144 tilted staves, each of which is made of two half staves with a total length of around 270 cm sitting at a radial position around 65 cm. AC-LGAD strip sensors are mounted on low mass Kapton flexible printed circuit boards (FPCs), and are wire-bonded with front-end ASICs. The FPCs are glued onto mechanical structures made from low density Carbon-Fiber (CF) materials, and bring power and input/output signals to the sensors and ASICs. The heat generated by the frontend ASICs are removed by an embedded Aluminium cooling tube in the CF structure. The FTOF consists of detector modules made from AC-LGAD pixel sensors bump-bonded with front-end ASICs. These detector modules are mounted from both sides onto a thermal-conductive supporting disk with embedded liquid cooling lines located around 190 cm away from the center of the experiment. Since the irradiation flux at the EIC is much smaller than that at the LHC, it is assumed that the radiation damage will not be a concern and the AC-LGAD sensors can be operated at room temperature.

**Sensors**: The sensors identified for the TOF timing layer are AC-LGADs that can provide both exceptional position resolution and timing resolution [3–6] while maintaining low channel density. The BTOF will employ strip sensors 1 cm long with a pitch of 500 um and a metal electrode width of 50 um (large pitch up to 1000 um is also under investigation). The sensor thickness will likely be 50 um to reduce the input capacitance to the pre-amplifiers but 30 um thick strip sensors are also under investigation. The full sensor size will be 3.2x2 $cm^2$ with 1 cm segments. The FTOF will employ pixel AC-LGADs with a pitch of 500 um and metal electrode size of 50 um (large pitch up to 1000 um and electrode size of 150 um are also under investigation). The thickness of the pixel sensors will likely be 20 um to maximize the time resolution reach, as the input capacitance is not a concern for small pixels. Nevertheless, 30 um thick pixel sensors are also under investigation. The full-size sensor will be 1.6x1.6 $cm^2$ with 0.5x0.5 $mm^2$ pixels. Studies on smaller-scale devices are presented in [3, 4]

and in the following. The full-size strip sensor prototypes have been produced for the first time in the most recent HPK fabrication and received at the time of writing. Procurement of the full-size pixel sensor prototypes is still in progress. A complete evaluation of the full size prototype sensors is expected in the middle/end of 2025.

**Front-End Electronics (FEE)**: The FEE for AC-LGAD based detectors is focused on the development of an ASIC and service hybrids. An ASIC featuring a Constant Fraction Discriminator (CFD) chip is being developed at Fermilab for the BTOF. The efforts have been focused on optimizing the analog frontend design to read out AC-LGAD strip sensors. Two versions of the ASICs, FCFDv0 and FCFDv1, featuring single- and multi-channel preamplifier and CFD, respectively, have been fabricated and tested. The new versions, FCFDv1.1 with further improvement to the frontend design tailored to 1 cm AC-LGAD strip sensors, FCFDv2 with digital readout, are under development with an expected deliver date in early 2025 and 2026, respectively. The EICROC project by the French group is focused on designing an ASIC for reading fine-pixelated AC-LGAD sensors, optimized pixel-based AC-LGADs detectors at ePIC such as B0, OMD, Roman Pots, and FTOF. The first version, EICROC0, is a 4x4 channel ASIC with 0.5x0.5 $mm^2$ pixel size, featuring components like a transimpedance pre-amplifier, 10-bit TDC for timing, 8-bit ADC for amplitude measurement, and an I2C slow control interface. It is designed for low capacitance and sensitivity to low charges (2 fC), operating with 1 mW per channel, and targeting 30 ps timing and 30 $\mu$ m spatial resolution. The prototype is currently under testing, with noise issues being addressed for future iterations. The next version, EICROC1 (expected in 2025), will feature a 16x8 channel configuration, followed by the final 32x32 channel version for full-scale implementation.

The service hybrids (SH) consists of a readout board (RB) and power board (PB). A schematic design of service hybrids, which serves 3 modules or 12 sensors/ASICs, for FTOF is shown in Fig. 8.5. The readout board will aggregate data from multiple ASICs to a lpGBT (from CERN) tranceiver chip via e-links, and then convert to optical signals via a VTRx+ chip (from CERN) to be transmitted to the backend data acquisition system. lpGBT and VTRx+ are designed for HL-LHC so have been proven to be sufficiently radiation hard for the EIC environment. The VTRx+ has one uplink up to 10 Gbs (for receiving clock and control signals), and four downlinks (for data transmission), each up to 2.56 Gbs, so it can transmit data up to four lpGBTs. The readout board also hosts interface connectors to the module board (as described later) and power board, as well as to input LV and BV cables. The power board provide low voltages for ASICs (1.2V), as well for lpGBT (1.2V) and VTRx+ (2.5V and 1.2V) on the readout board via DC-DC converters. The CERN bPOL48V module is chosen as the main converter, which takes an input of 15V and converts it into 1.2V and 2.5V. As illustrated in Fig. 8.5, the RB is situated on top of the PB and sensor module. The PB is directly contacting the cooling structure to facilitate efficient cooling of heat dissipation from DC-DC converters. The SH will have three different types with different lengths, serving 3 (12), 6 (24) and 7 (28) modules (sensor/ASICs). This will provide the most efficient coverage of a circular shaped disk while minimizing number of cables and fibers. The example shown in Fig. 8.5 is the shortest version (about 100mm long) which serves 3 modules. The latest layout design for FTOF disk is shown in Fig. 8.2 (right), where different colored boxes indicate different types of SHs. Prototyping of the SH is in an advanced stage. A pre-prototype readout board (ppRDO) has been developed and under testing, based on an Xilinx FPGA chip and a commercial SFP+ optical transceiver. The first prototype RB and PB based on CERN chips will be soon developed, especially based on similar existing design of the CMS endcap timing layer (ETL) detector.

**Flexible Printed Circuit boards**: The Flexible Printed Circuit (FPC) is used to read out data and distribute power to the sensors and ASICs. In the acceptance region, a material budget of 1% $X/X_0$ is required, meaning the FPC material should be as minimal as possible. Ad-

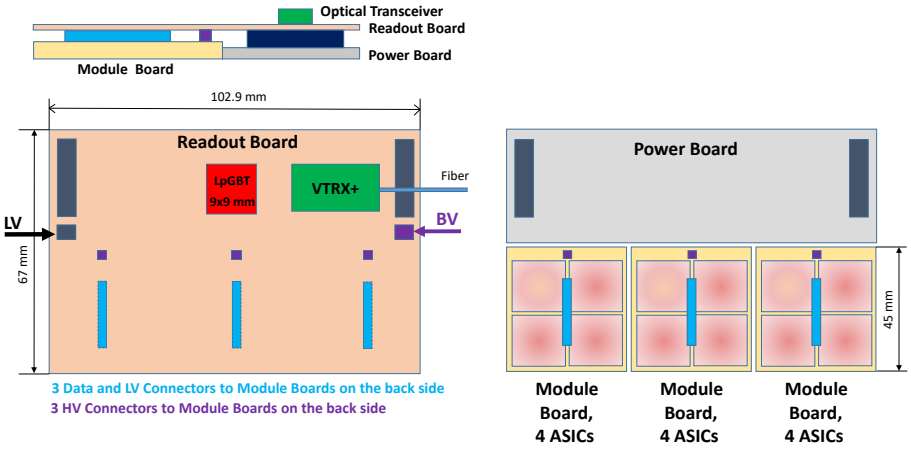


**Figure 8.5:** A schematic design of service hybrids for FTOF, which serves 3 modules or 12 sensors/ASICs.

ditionally, the FPC must be 135 cm in length. To meet these stringent requirements, careful consideration of the FPC material is necessary, as signal loss is expected with such a long FPC, especially if using polyimide, a standard material in FPCs. The sPHENIX experiment encountered a similar challenge with their Inner Tracker (INTT), a silicon sensor tracker, and successfully addressed it by using Liquid Crystal Polymer (LCP) instead of polyimide as the dielectric material. This technology will be adopted for our detector as well.

**BTOF stave design**: Barrel staves are divided into two half-staves, with services and connections coming from the outer side. The half-staves consist of a support structure with an integrated cooling pipe, flexible printed circuit (FPC), sensors, and ASICs. Sensors and ASICs are mounted on both the front and back sides of the half-stave, making it double-sided, with enough overlap to achieve 100% coverage in the stave direction. The lateral overlap and tilting ensure 100% coverage in the direction parallel to the staves. In total, there are 64 sensors and 128 ASICs on each side of the half-staves.

**FTOF module design**: A schematic design of the module for FTOF is shown in Fig. 8.6. Each module consists of $2 \times 2$ LGADs sensors and ASICs. It is covered by a module PCB board (MB), which will provide LV power (1.2V) and transmit the data of ASICs via a board-to-board connector to the RB. In addition, the MB also has a BV connector to the RB for providing the BV to LGADs sensors. ASIC readout will be wire-bonded to a metal pad near the edge of the module on the side facing the baseplate and cooling structure, as illustrated in Fig. 8.6 (right). LGADs sensor and ASIC will be connected via bump bonding. Dimensions shown are preliminary and will be adjusted as the prototyping progress. In the current design, the LGADs sensor is placed underneath the ASIC. The motivation is to have the sensor as close as possible to the cooling structure to ensure lower and stable temperature, which has been proven to be essential for achieving optimal time resolution. An alternative option would be to swap the ASIC and sensor layer, which has the advantage of more efficiently dissipating heat primarily generated by the ASIC. A final choice will be made as the prototype progress, especially after realistic thermal performance studies have been carried out.

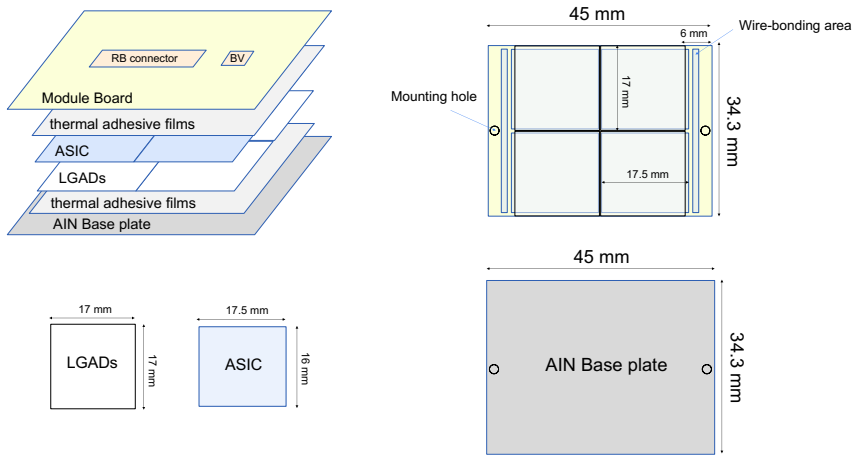


**Figure 8.6:** A schematic design of the module for FTOF, which consists of $2 \times 2$ LGADs sensors and ASICs.

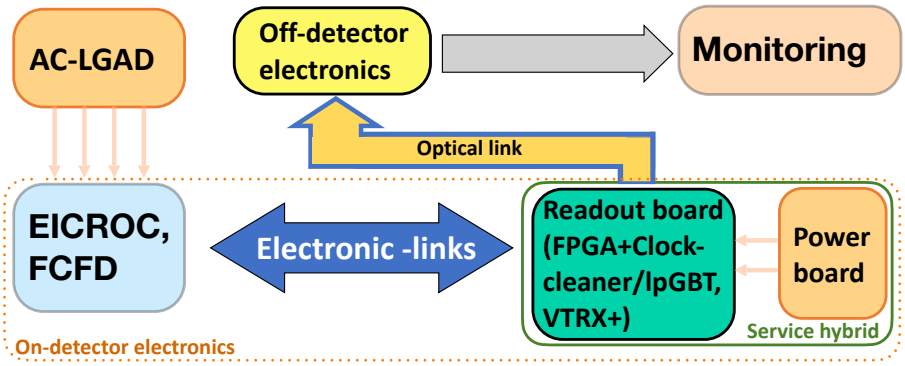


**Figure 8.7:** Schematic of the AC-LGAD sub-system readout chain. Each component is undergoing design, (pre-)prototyping, testing under various environments, and customization to meet the specific requirements of individual subsystems.

**Performance** The AC-LGAD systems, including the BTOF, FTOF, and far-forward systems (Roman Pots, OMD, and B0 tracker), share a common readout chain currently under development. Performance evaluations are being conducted in various laboratory environments as part of the ongoing R&D efforts. A schematic of the full readout chain is shown in Fig. 8.7. The effort can be divided into to parts: 1) integrating the sensors with ASIC, 2) development of the readout-board and power board.

The Fermilab team has been developing an ASIC targeting the AC-LGAD strip sensors for BTOF. Studies showed that Constant Fraction Discriminator (CFD) could provide a better timing resolution with small signal amplitude from LGAD than leading edge descriminator [7]. The first single-channel CFD-based ASIC (FCFDv0) wire-bonded to a DC-LGAD sensor achieved 35 ps timing precision with beam, where the dominant contribution is expected from the intrinsic resolution of the LGAD sensor. A 6-channel prototype (FCFDv1) was developed for AC-LGAD sensors, demonstrating 11 ps jitter in charge injection and 50 ps time resolution with 0.5 cm AC-LGAD strip sensor

in test beam. Ongoing efforts are focused on optimizing the frontend design for 1 cm AC-LGAD strip sensors for the BTOF.

Assemblies of 4x4 AC-LGAD pixel sensors with $500 \times 500$ $\mu m^2$ pixelation and 30 $\mu$m thickness, and 4x4 EICROC0 ASICs, were completed by the BNL, IJCLab, OMEGA, and Hiroshima groups on test-boards developed by IJCLab/OMEGA. Testing included scans of the analog and digital components using charge injection and beta particles from a Sr-90 source, resulting in a measured jitter of 8-9 ps for charges above 20 fC. Both wire-bonded and flip-chip assemblies were developed for various characterizations. Additional tests using Transient Current Technique (TCT) laser scans were conducted to map out charge distribution, and various tests are still ongoing.

ORNL is developing flexible Kapton PCBs for TOF applications, where sensors and mockup ASICs will be glued, wire-bonded, and co-cured onto a composite structure at Purdue for evaluation. Flip-chip options will be available soon, aiming to support low-cost sensor-ASIC hybridization techniques.

In FY24, BNL, LBNL, and Rice developed a prototype board (ppRDO) for precise clock distribution and ASIC integration for AC-LGAD systems. Key milestones, including schematic designs, part orders, PCB layout, and initial testing, were completed ahead of schedule. Firmware development and performance tests on clock-cleaning, jitter, and power distribution are ongoing. The collaboration aims to continue in FY25, focusing on the development of a readout board (RBv1) and power board (PBv0) for AC-LGAD systems, supporting TOF applications and ensuring DAQ compatibility. The ppRDO includes three components: 1) FPGA, 2) clock cleaner, and 3) SFP+ module. Future versions will adopt lpGBT to replace the FPGA and clock cleaner, and VTRx+ to replace the SFP+ module, improving performance, radiation hardness, and integration.

### Implementation

**Services:** Electric power is distributed to the detector components via the Power Board (PB), which is part of the Service Hybrid (SH). The SH also includes the functionality of the Readout Board (RDO). In the case of BTOF, one SH supports 64 sensors and 128 ASICs, with SHs placed on both sides of the stave. For FTOF, several types of SHs are used, covering 12, 24, or 28 sets of sensors and ASICs. The SH is distributed on the mechanical and support disk, together with sensor modules.

Low Voltage (LV) and High Voltage (HV) cables are connected to the PB, where multiple DC-DC converters step down or adjust the voltages as needed. HV is applied to groups of multiple sensors, rather than distributed individually to each sensor. The size of each sensor group is determined by the design of the sensors and the electronics. Table 8.3 summarizes the service (cables and tubes) necessary for TOF detectors.

A liquid cooling system is employed to control the temperature of the detector. For the BTOF stave, one or two cooling pipes are integrated into the stave sandwich structure, with liquid flowing in one direction along the length of the stave. In FTOF, a winding liquid pipe is integrated into the support sandwich structure. The flow rate and pipe diameter are determined by the amount of heat generated and the detector's performance requirements, thermal finite element analysis determines the design. The pressure must remain below the surrounding air pressure to ensure safe operation. Fig. 8.8 shows a single BTOF stave with cooling pipe (left) and half of the FTOF structure with cooling pipes (right).

| **subsystem** | item | quantity | diameter (mm) | lengths (m) | description |
|---|---|---|---|---|---|
| BTOF | 288 FEE LV s.hybrid dist. | 24 | 20 | 15–25 | Rack to Panel, 8AWG(24 AWG sense pairs) |
| BTOF | FEE LV | 72 | 6.3 | 8 | panel-to detector, Alpha-PN: 2424C SL005 |
| BTOF | FEE HV | 18 | 14 | 15–25 | Rack to Dist. Panel |
| BTOF | FEE HV | 144x2 | 1.5 | 8 | panel to sensor |
| BTOF | cooling tubes | 144x2 | 5 | $> 2.6$ | supply/return from panel to stave (Aluminum) |
| BTOF | cooling tubes | 4x2 | | | supply/return to panel |
| FTOF | 132FEE/ sHybrids, service feeds | 44 | 10.0 | 25 | LV,rack-to-detector LV-dist,14AWG TC,w/24AWG-sense wires |
| FTOF | 132FEE/ sHybrids, dist. | 44 | 9 | 3 | 18 AWG TC, 6 cond.dist. panel-to s.hybrids |
| FTOF | FEE HV | 212 | 2.42 | 10 | panel to sensor |
| FTOF | cooling tubes | 2x2 | 5 | | supply/return from panel to detector (Aluminum) |
| FTOF | cooling tubes | 2 | | | supply/return to panel |

**Table 8.3:** Summary of BTOF and FTOF low voltage and high voltage power supply cables to distribution panels and then to the detector FEE (the exact numbers are being checked at the time of writing).

**Subsystem mechanics and integration:** Both the BTOF and FTOF detector systems are supported by their own support structure, which is integrated and supported by the global support tube (GST). The BTOF is a barrel geometry time-of-flight detector system located at a radius of 63cm from $z = -117.5$cm to $z = +171.5$cm along the beam direction as shown in Fig. 8.9. Both detector subsystems have 7.5cm space in radial direction for BTOF and in the beam direction for FTOF. The three engagement rings (each of 5mm width) are made from composite materials as a sandwich and support the BTOF detector - they are itself supported by the GST. A first concept was developed for a BTOF stave mounting mechanism employing the engagement rings by clips with staves at an 18 degree angle. Staves are removable individually to ease maintenance. The FTOF detector is designed in two half disc structures, or dee's, that are kinematically mounted to the GST. Services (readout, power, cooling) of the BTOF and FTOF are routed either way and supported itself by the GST. Table 8.4 lists the positions of BTOF and FTOF relative to the global ePIC geometry.

**Calibration, alignment and monitoring:** **Calibration and alignment:** For spacial calibration and alignment, the TOF layer is essentially treated as a layer of the overall tracking system. There-

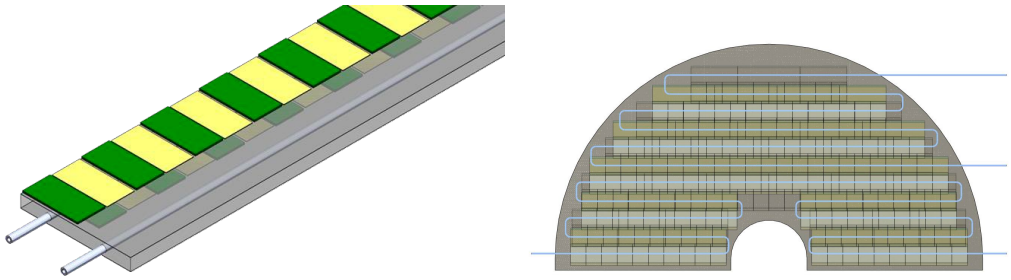

**Figure 8.8:** schematic drawings of one BTOF stave (left) and half of the whole FTOF (right) cooling pipes.

| **subsystem** | $z_{min}$ (cm) | $z_{max}$ (cm) | inner radius (cm) | outer radius (cm) | stave angle |
|---|---|---|---|---|---|
| Barrel TOF | -117.5 | 171.5 | 62 | 69.5 | $18^o$ |
| Forward TOF | 185 | 192.5 | 10.5 | 60 | 0 |

**Table 8.4:** BTOF is designed with a barrel geometry surrounding the beam pipe and interaction point, while FTOF is a disk geometry perpendicular to the beam direction on the hadron side (positive $z$).

fore, spacial alignment will be carried out as part of the entire tracker. This is typically based on the match between tracks reconstructed in other layers of the tracking, then extrapolated to the TOF and the hits in the TOF. By combining the information from many tracks, high precision can be achieved.

To exploit timing in the reconstruction of the charged tracks, the different TOF channels will have to be synchronised to a precision of a few picoseconds. The absolute time calibration (or phase shifts relative to the beam clock) is not a particular concern, as all the event reconstruction relies on the relative time between tracks within the same collision event. The time offsets of the TOF channels can be inter-calibrated using all the tracks collected online through a fast reconstruction stream. The distribution of the reconstructed time at the vertex of these tracks – assuming they are pions – should an rms spread of approximately 50 ps, including the time spread of the luminous region and detector resolution. The mean time of this distribution over many tracks provides the reference calibration points. Non-pion particles will contribute to the tail of the distribution, which can be cleaned up using an iterative procedure but not necessary. These calibrations can be made available for the prompt reconstruction of the events and updated frequently.

**Monitoring:** In the readout scheme of the TOF, a common clock is distributed to the individual channels belonging to the same service hybrid. The time stability of the clock distribution can be monitored with a precision of a few ps every second.

### Status and remaining design effort: eRD112 and eRD109

**eRD112: Sensor R&D effort** A brief summary of eRD112 activities is reported in this section, for a more detailed review of the sensor development effort consult the 2024 erd112 report document. HPK sensors from the latest production have been tested at the Fermilab test beam facility; the results are summarized in Ref. [4]. The summary best results are reported in Fig. 8.10. The same HPK production was tested in laboratory with focused laser TCT and showed similar results as

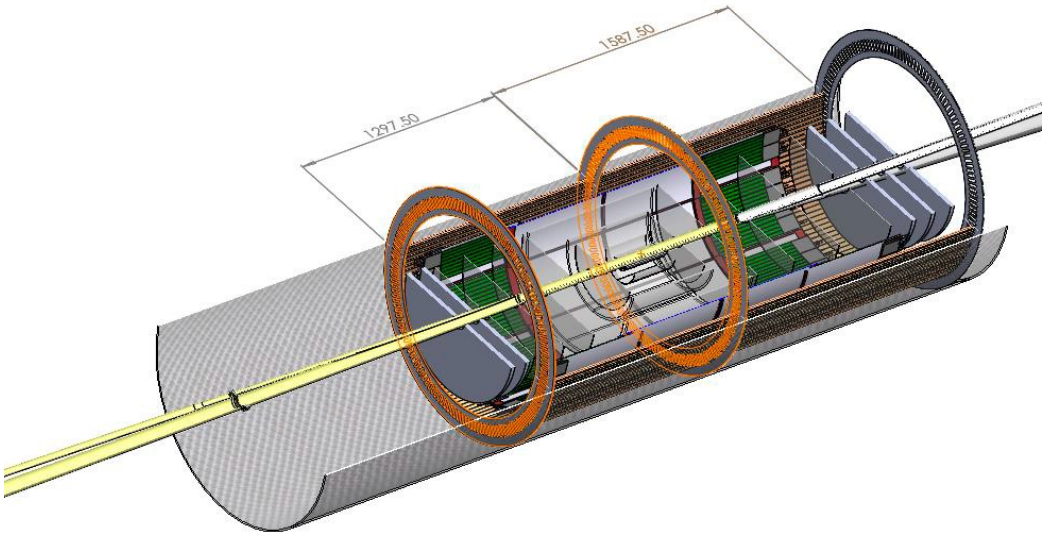


**Figure 8.9:** Barrel TOF supporting mechanic structure with engagement rings situatued and supported by the EPIC global support tube structure (GST). The width of each of the three engagement rings is 5mm.

reported in Ref. [5]. The presented strip sensors (Fig. 8.10, Left) show a constant time resolution of around 35 ps, which is within the requirements for the ePIC TOF. The strip reconstructed position resolution is between 10-20 $\mu m$, which is also within the ePIC TOF requirement of 30 $\mu m$. The best result for pixel sensors (Fig. 8.10, Right) shows an homogeneous time resolution of 20-25 ps, well within ePIC TOF requirements. The position resolution instead is 20-70 $\mu m$ across the device; the charge-sharing mechanism allows for precision reconstruction in between metal electrodes, but the resolution is significantly worse for hits directly on the metal electrodes.

The position resolution requirement for the FTOF is 30 $\mu m$. Therefore, pixel technology needs to be refined to meet the requirements. The new HPK production (expected by the end of the year) includes smaller electrode sizes and larger gaps between electrodes that could provide good reconstruction across the sensor. However, it was observed that a larger gap decreases the total S/N between electrodes, which might degrade the overall performance of the sensors. Results from a BNL production provide a promising alternative to square metal pixels. The S/N is better across the sensor for a cross-shape electrode given the same central metal shape, allowing for better reconstruction using charge sharing. HPK did not include cross-shape geometry in the latest production, but it might be included in the next one. Another producer of cross-shaped AC-LGADs is Fondazione Bruno Kessler (FBK). The FBK prototypes were investigated with a laser TCT, and a similar behavior was observed for cross-shaped devices [6].

The sensors irradiated at the Triga Reactor with 1 MeV neutrons were received in Spring 2024 and characterized both for electrical proprieties (capacitance and current over voltage) and with the laser TCT station. Gain degradation can be probed with measurements of capacitance over voltage by identifying the gain layer depletion point ($V_{GL}$). Fig. 8.11, Left, shows the change in the gain layer for the irradiated HPK AC-LGADs from several wafers, with different N+, oxide and active thickness, up to $1 \times 10^{15}$ Neq; in the region of interest for ePIC $< 10^{13}$ Neq the gain layer is un-

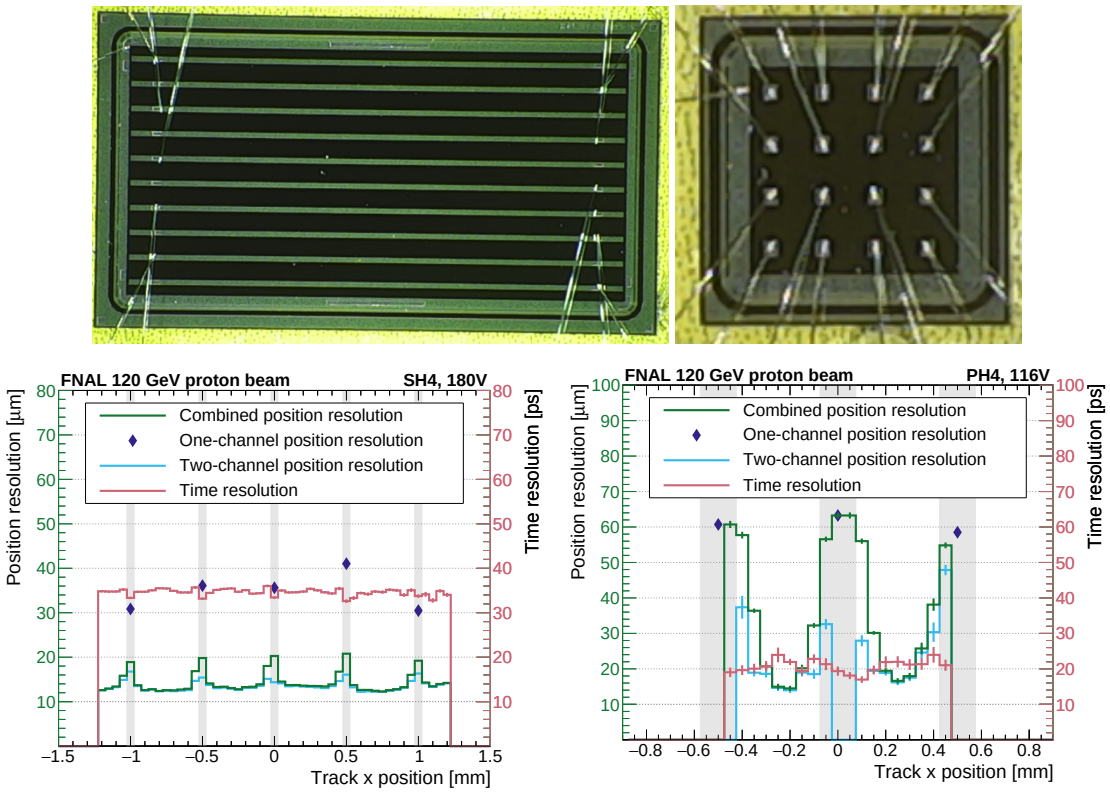


**Figure 8.10:** Left: Picture and beam test results for HPK strip sensor, 1 cm long, 500 $\mu m$ pitch, and 50 $\mu m$ metal electrode width. Right: Picture and beam test results for HPK pixel sensor, 4x4, 500 $\mu m$ pitch, and 150 $\mu m$ metal electrode width. Plots from Ref. [4].

changed. The charge-sharing proprieties after irradiation were tested using a focused IR laser in the laboratory. As seen in Fig. 8.11, Right, the spatial response of the sensor is unchanged after irradiation up to $5 \times 10^{14}$ Neq. The current increase in the irradiated HPK sensors is also negligible until $< 10^{13}$ Neq, as shown in Fig. 8.11, Bottom. The measurements were done at room temperature; therefore, no cooling will be necessary to reduce the dark current, which would increase the sensor power dissipation in ePIC. In conclusion, no change in the behavior of the sensors is expected during the lifetime of the ePIC detector due to radiation damage.

**eRD109: readout R&D effort** A more detailed review of the electronics development effort can be found in the 2024 eRD109 report document. In the following section, a brief summary will be provided.

The Fermilab team has continued the development of the FCFD ASIC prototype and, in FY23, has designed the first multi-channel prototype with this approach, labeled as FCFDv1. Numerous technical improvements were implemented based on the experience with FCFDv0, aimed at addressing the stability and performance of the system. The FCFDv1 ASIC was submitted for production in September 2023, and received in January 2024. A specialized readout board was designed to accommodate the FCFDv1 connected to a 0.5 cm HPK AC-LGAD strip sensor. Initial measurements of the performance were done using internal charge injections performed with an LGAD-like signal. With input capacitance ~3.5 pF a jitter of around 11 ps was achieved, as shown in Fig. 8.12, left. Test beam campaigns have been performed to study the performance of the FCFDv1 in June

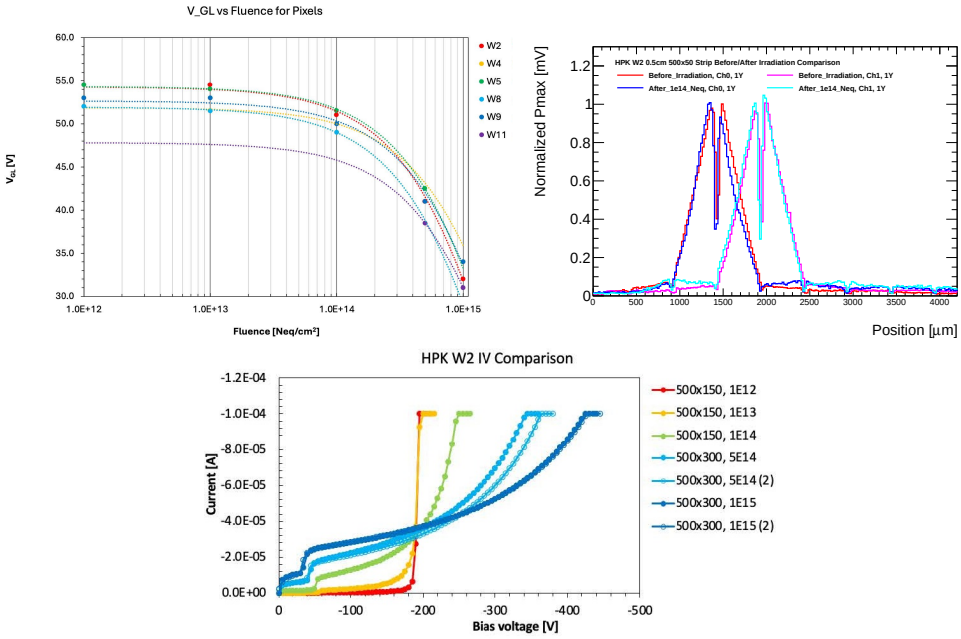


**Figure 8.11:** Left: Degradation of the gain layer for AC-LGADs of several wafer (with different N+, oxide and active thickness) from HPK latest sensor production, showing no change in gain layer doping up to $10^{13}$ Neq, which is an order of magnitude over the ePIC TOF radiation requirement. Sensors were irradiated at the TRIGA reactor (Lubjiana) with 1 MeV neutrons. Right: Normalized comparison of response profile of two nearby strips for two HPK 0.5 cm length, 500 $\mu m$ pitch, 50 $\mu m$ strip width: one before irradiation and one after $1 \times 10^{14}$ Neq, even if the total signal is degraded the charge sharing profile is unchanged. Bottom: Current over voltage measurement for irradiated HPK sensors.

2024. The newly introduced amplitude readout was found to function well, and results show 100% efficiency when combining neighboring strips. The time resolution measured from the beam test was around 50 ps. A further design improvement is foreseen in FCFDv1.1 to accommodate 1 cm AC-LGAD strip sensor and improve the timing resolution.

The development of the EICROC0 chip is proceeding as planned. In 2024, an updated PCB ("2024" PCB), has been designed by OMEGA. This updated PCB features improved testability and grounding, as well as the removal of supplementary PLLs. The chip shows good homogeneity between channels and Jitter $<$35 ps for an injected charge of $>$4 fC, both for the pre-amplifier and for the discriminator output, as seen in Fig. 8.12, Left. A large correlated noise still remains with the updated "2024" PCBs (already observed in the "2023" PCB), which leads to large TDC jitters, over 50 ps, when by design, the TDC jitter is expected to be of the order of 10 ps. Nevertheless, the intrinsic performance of the preamplifier, the TDC, and the ADC, taken individually, is confirmed to be in agreement with the design and within the ePIC detector specifications.

The development of pre-prototype readout board (RDO) with high precision clock distribution has been completed. Figure 8.13 shows a picture of the ppRDO. It is connected with the CMS ETL module board v0, which consists of the full-sized ETROC2 chip for testing purpose. The ppRDO will be evolved into the prototype RB for FTOF next that consists of lpGBT and VTRx+ chips, instead of FPGA and SFP+. Those efforts will be carried out under engineer designs as described later.

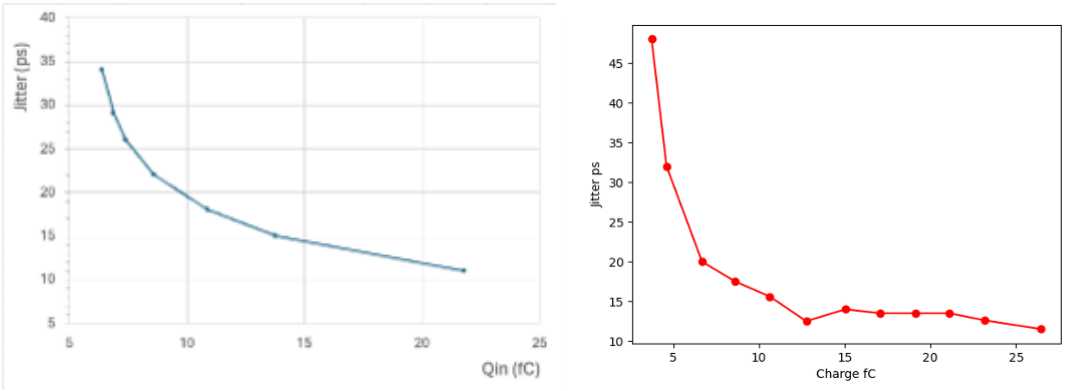


**Figure 8.12:** Left: FCFD Jitter measurements with 3.5 pf input capacitance and charge injection. Right: EICROC Discriminator jitter versus the injected charge, determined from data on an oscilloscope. Left: FCFD Jitter measurements with 3.5 pf input capacitance and charge injection. Plots from the erd112 and erd109 2024 reports.

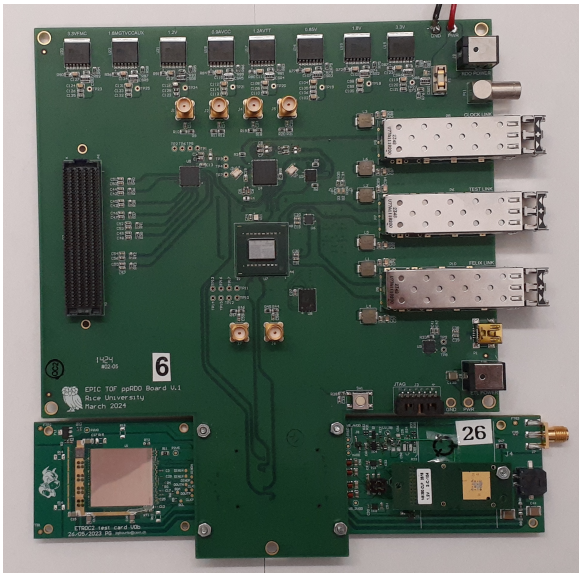

**Figure 8.13:** Picture of ppRDO connected with CMS ETL module board v0 for testing.

**E&D status and outlook:** E&D activities

**Thermo-Mechanical demonstrator:** The fabrication of a demonstrator stave following the double-sided design, as seen in Fig. 8.15, is ongoing. The demonstrator will be a thermal/mechanical demonstrator of the assembly procedure and chip/sensor power dissipation. A mock-up stave, example in Fig. 8.14, will be co-cured with a readout flex with a cooling pipe in the center, and a series of Si heaters and full-size HPK sensors from the latest production will glued to the stave, then wire-bonded together and to the readout flex. The demonstrator will be used to probe the power dissipation, the temperature gradient across the stave, and the mechanical assembly procedure. Demonstrator results are expected by Q1 2025.

**Figure 8.14:** Assembled stave prototype at Purdue.

**Environmental, Safety and Health (ES&H) aspects and Quality Assessment (QA planning):** We also carried out QA long-term and stress-test reliability studies of LGADs as a stepping-stone towards studies on AC-LGADs. The tests were conducted in an ambient chamber at various environmental conditions. We kept the sensors under bias voltage over periods of weeks, at different temperatures, ranging from -60 to +80 degrees Celsius and under different humidity conditions. Under these extreme conditions we carried out I-V scans. At intervals of time between temperature cycles, we also collected signals from beta particles from a Sr-90 source at room temperatures to study any deterioration in noise or charge collection. The results were presented at IEEE conference: While we saw an impact of humidity and temperature on current and breakdown voltage, the sensors recovered their original performance in subsequent cycles. In addition, we also studied the impact of passivation on sensors to minimize charge build-up and early mortality. We confirmed that passivation is critical to minimise the impact of humidity on sensors and prevent early mortality. Such tests were critical after issues have been observed in silicon sensors used for tracking detectors in other experiments, such as those at the HL-LHC. As part of our QA strategy, we also sent to colleagues of UNM BNL-made AC-LGADs to have them irradiated at various fluences in a proton beam at ITA, in a gamma beam at SANDIA and with neutrons at the TRIGA reactor. The first results are shown in the previous sections.

For both sensors and readout chips, it is imperative to evaluate the yield of the test productions to adjust the final production orders. The QA plans to evaluate the yield of the sensor productions are as follows: each produced sensor will be tested in the laboratory in a probe station with simple current over voltage (IV) and capacitance over voltage (CV) tests. AC-LGADs have a single point of DC connection on the N+, so only 1 or 2 needles are necessary for the test; a probe card is not necessary for QA. The IV test will allow us to check the current level and the breakdown voltage for each produced device; the current level has to be $<< 1\mu A$ to not introduce power dissipation issues. The breakdown voltage of all devices has to be within **10%?** to avoid issues in the HV distribution. The CV test will allow to probe the gain layer depletion voltage and demonstrate that all devices have homogeneous gain; for LHC prototypes[2], the gain homogeneity was within 1%. A selection of devices from the full production will be characterized by mounting them on analog front-end boards with laser TCT and at test beam facilities to ensure the homogeneity of the charge-sharing response.

To evaluate the yield of the chip (EICROC, FCFD) productions, a sample of chips from each batch will be tested and probed for homogeneity in all the channels using a calibration input. All channels have to be within **10%?** of homogeneity. A selection of chips will be coupled (wire bonded or bump bonded) with a matching working sensor and mounted on a prototype PCB to probe correct and homogeneous operation in a realistic configuration. Then the boards will be tested with a laser TCT or at test beam facilities.

Once the state of sensors, readout chips, and flex is advanced, a fully loaded demonstrator stave is envisioned. The mounting procedure will already be tested during the assembly of the thermo-mechanical demonstrator. The full demonstrator will then be tested with radioactive sources in laboratory or at test beams.

**Construction and assembly planning:** The BTOF detector has a cylindrical shape, consisting of 144 tilted staves. These staves are assembled at designated sites within class-7 or higher clean rooms before being transported to BNL for final construction. Each stave is approximately 270 cm long and is divided into two half-staves of 135 cm. A half-stave includes a support structure with an integrated cooling pipe, a flexible printed circuit (FPC), sensors, and ASICs. The sensors and ASICs are mounted on both sides of the half-stave, with 64 sensors and 128 ASICs on each side. Wire-bonding is used to connect the ASICs to the sensors and electronics. Only components that pass various quality inspections—such as visual checks, metrology, and electrical tests—proceed to the assembly stage. During the half-stave assembly, one FPC is glued onto the support structure (Fig.8.15 (a)). To ensure precise alignment, a specialized tool is used, featuring pins and holes that guide the placement of the FPC and the correct application of glue. After assembly, the staves undergo both electrical and mechanical tests. Subsequently, sensors and ASICs are installed on the FPC surface using alignment tools similar to those used during the FPC mounting process (Fig.8.15 (b)). These tools help position the components and apply adhesive. Electrical connections are verified, and the ASICs are bonded to the sensors using wire-bonding, followed by wire encapsulation (Fig.8.15 (c)). 2 support structure with wire-bonded sensor, ASIC, FPC which is corresponding to front and back side, are attached to each other (Fig.8.15 (d)). Upon completing the installation on both sides (Fig.8.15 (e)), the final round of testing is conducted. Fully tested staves are then shipped to BNL for integration into the global support structure of the ePIC detector, which contains 144 slots for precise alignment of the staves within the global coordinate system.

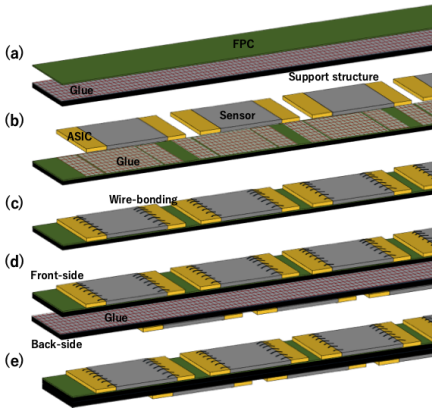


**Figure 8.15:** Assembly process of BTOF stave. Note, the scale is not real.

The FTOF is constructed in a double-sided disk shape by populating modules with dimensions indicated in Fig. 8.6. Each module includes 4 sensors, 4 ASICs, a module board, and an Aluminum Nitride (AlN) base plate, which acts as a thermal conduit to the cooling system. The modules are connected to a service hybrid (SH) that consists of a power board (PB) and a readout board (RB). As mentioned earlier, three different configurations of SH are used, depending on the number of modules being supported: 3 modules (RB3), 6 modules (RB6), and 7 modules (RB7). There are about 780 modules in total to patch the disk shape. Sensor and ASIC are connected by bump-bonding. The module board is connected to the ASICs through wire bonding and has a connector to interface with the RDO. Assembly of the modules occurs in class-7 (or higher) clean rooms, while the PB and RB can be assembled under standard conditions. The assembly of each module begins with the connection of one sensor to one ASIC using bump-bonding technology (Fig.8.16 (a)). Automated machines are used for sensor and ASIC placement, alignment, and bonding. After bonding, the electrical performance of the sensor-ASIC hybrids is tested. Following this, 4 sensor-ASIC hybrids are mounted on the module board, using a dedicated tool to ensure precise alignment

(Fig.8.16 (b)). Thermal adhesive films are placed between the hybrids and the module board to ensure efficient heat dissipation. Once mounted, the ASICs are wire-bonded to the module board, and the wires are encapsulated for protection. After the bonding process, the AlN base plate is attached to the opposite side of the hybrid (Fig.8.16 (b)), with thermal adhesive films again used between them to aid heat transfer. The thermal adhesive films are also put between them. The modules undergo thorough quality checks before moving on to SH assembly. The RBs and PBs are manufactured using standard circuit board techniques and come with dedicated connectors for integration. SHs are available in configurations supporting 3, 6, or 7 modules, with the RB and PB connected via dedicated interfaces (Fig.8.16 (c)). Once assembled (Fig.8.16 (d)), the modules and SHs are tested for connectivity and performance. After passing all tests, the modules and SHs are shipped to BNL, where they are attached to the disk-shaped support structure. Specialized tools ensure the accurate placement of the components. Modules and SHs are mounted on both sides of the support structure to eliminate acceptance gaps between sensors. When installing the modules and SHs on the opposite side, a fixture is used to maintain the required clearance between components. Finally, the fully assembled disk is installed into the ePIC detector.

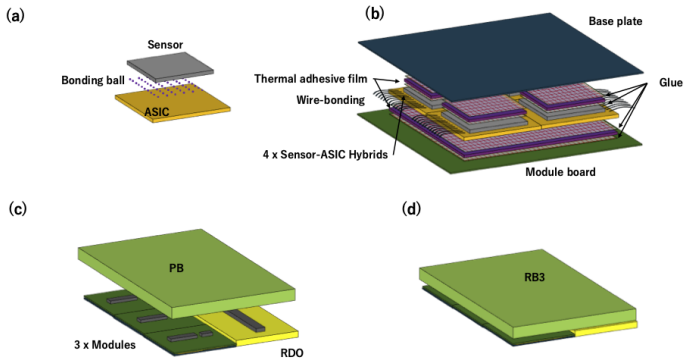


**Figure 8.16:** Assembly process of FTOF modules. RB3 type is shown as an example. Note, the scale is not real.

**Collaborators and their role, resources and workforce:** Table 8.17 shows the participating institutes with their role, the contact person and potential commitments. This shows substantial participation by the international collaborators outside of the U.S.. We also anticipate substantial funding support from the international collaborators for the BTOF detector as well.

**Risks and mitigation strategy:** Our R&D results (eRD112) show that the performance of the sensors would meet physics requirements for TOF subsystems. Those studies were done with smaller chip dimension. The production for R&D study with full-size sensor chip is underway. There is a potential risk that the performance of sensors with larger size would be worse. The mitigation is to reduce the sensor size.

The HPK sensors for R&D (eRD112) is of small quantity. A mass production would be a risk in terms of chip yield and schedule delay. The mitigation is to explore other possible production sites (Taiwan/FBK).

FCFD ASIC design (eRD109) currently only has analog signal readout. The design and test of the digitization component is underway and expected to have first pass early next year. Addi-

| Institute | Contact Person | NOW (TDR->Project) |
|---|---|---|
| Brookhaven National Laboratory | Prithwish Tribedy tribady@bnl.gov | DAQ readout chain readout, sensor-ASIC integration, sensor with FF AC-LGAD; EICROC testing |
| Fermi National Accelerator | | FCFD ASIC (no ePIC) |
| Los Alamos National Laboratory | Xuan Li xuanli@lanl.gov | |
| Rice University | Wei Li wl33@rice.edu | B/FTOF FEE?, Backend electronics (postdoc) , simulation and reconstruction |
| Oak Ridge National Laboratory | Oskar Hartbirch hartbricho@ornl.gov | sensor-ASIC integration, frontend electronics (waffle probing), module assembly |
| Ohio State University | Daniel Brandenburg Brandenburg.89@osu.edu | BTOF/FTOF: module assembly; backend electronics |
| Purdue University | Andreas Jung anjung@purdue.edu | Module assembly |
| Univ. of California, Santa Cruz | Simone Mazza simazza@ucsc.edu | Sensor, sensor-ASIC integration, module assembly (no in-kind) |
| University of Illinois at Chicago | Olga Evdokimov mailto:evdolga@uic.edu | |
| Hiroshima University | Kenta Shigaki shigaki@hiroshima-u.ac.jp | FTOF EICROC testing, sensor testing (30%), simulation |
| RIKEN | Yuji Goto. goto@bnl.gov | BTOF: module assembly |
| Shinshu University | Kentaro Kawaide kawade@shinshu-u.ac.jp | Sensor testing, simulations |
| University of Tokyo | Taku Gunji gunji@cns.s.u-tokyo.ac.jp | DAQ streaming readout |
| South China Normal University | Shuai Yang syang@scnu.edu.cn | |
| Univ of Sci. and Tech. of China | Yanwen Liu | |
| Indian Institute of Tech., Mandi | Prabhakar Palni prabhakar.palni@unigoa.ac.in | FTOF Module Assembly/QA, sensor testing |
| National Inst. of Sci. Edu. Res. | Ganesh Tambave ganesh.tambave@niser.ac.in | Module Assembly |
| National Central University | | FF AC-LGAD (sensor QA) |
| National Cheng-Kung University | Yi Yang yiyang@ncku.edu.tw | Mechanics and cooling systems |
| National Taiwan University | Rong-Shyan Lu rslu@phys.ntu.edu.tw | FF AC-LGAD; module assembly |
| Univ. Técnica Federico Santa María | | Simulations |
| LBNL | Zhenyu Ye yezhenyu2003@gmail.com | BTOF ASIC testing; SH |
| Kent State University | Zhangbu Xu zxu22@kent.edu | Simulation, readout test, machine shop (in-kind) |
| Nara | Takashi Hachiya hachiya@cc.nara-wu.ac.jp | BTOF module assembly/validation/FPCB |

**Figure 8.17:** Collaboration institutions and their responsibilities.

tional resource may be need to mitigate potential schedule delay and cost increase. In addition to the baseline chips EICROC and FCFD, third-party ASICs are also taken into consideration: FAST (INFN Torino), AS-ROC (Anadyne Inc. + UCSC), and HPSoC (Nalu + UCSC). The most advanced one is the High-Performance System-on-Chip (HPSoC) ASIC, designed by Nalu Scientific [8], in close collaboration with SCIPP, and fabricated in 65 nm CMOS by TSMC. HPSoC comprehends a fast analog front end and, unique to all other current LGAD readout ASICs, will capture the full signal waveform at a sampling rate of 10-20 GS/s. Together, these are expected to address the EIC goal of 25 ps timing resolution or better per measured space point. V2b of the chip has a working digital back-end and is currently under review.

We have performed heat conductivity and cooling simulations, and R&D test on cooling capacity (currently with PED funding). Those show promising outcome for meeting the cooling needs. The potential risk is that the cooling capacity is not sufficient to maintain a stable and relatively uniform temperature. A possible mitigation strategy is to use different material for cooling pipe with better heat conductivity and higher flow rate.

**Schedule** The schedules for BTOF and FTOF projects are shown in Fig.8.18. A major inter-dependence of the schedule is the sensor and ASIC designs. In the preproduction phase, 10%

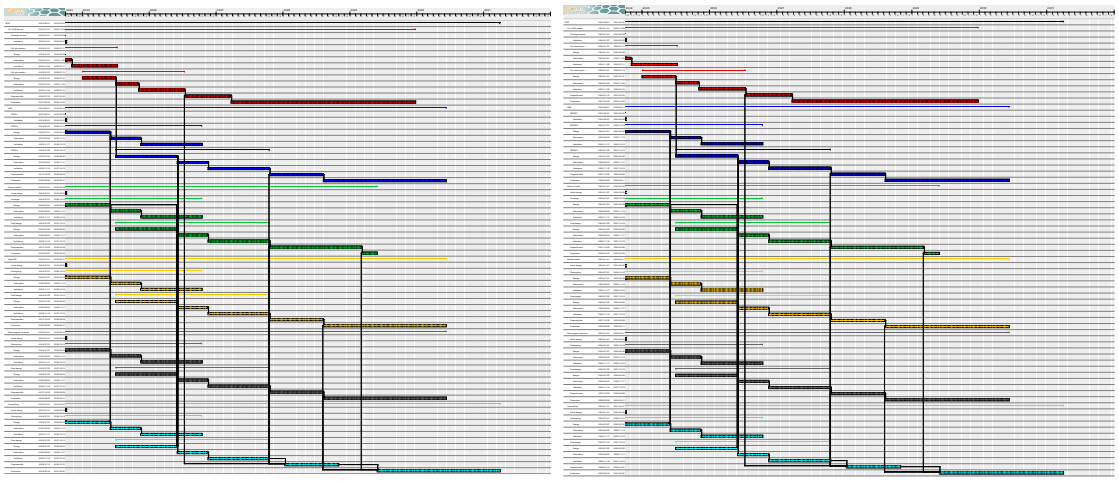

**Figure 8.18:** Schedule of BTOF and FTOF projects (2024/10/05 version.)

will be made in six months while quality and procedures are being confirmed in this period. Then, during the Production phase, the remaining 90% will be produced in two years.

### Additional Material

**Low-voltage and High-Voltage powersuplies** Each service hybrid module will be powered by a radiation and magnetic field tolerant DC-DC regulation board as part of the hybrid module and mounted to the cooling plate. The minimum efficiency of the regulator board should be $\geq$ 70.0%. Input power to the DC-DC board is delivered from rack-mount Wiener PL500 series power supplies to source 15 Volts DC $\pm$ 3.0%. The current demand from the rack-mount PSU should not exceed 80.0% of the manufacturers rating. Each channel of the PSU will have over-current fuse protection. The power cabling size is selected to operate at 125% of the total continuous maximum load. The estimated power consumption and LV cable feed size for each detector is designated as follows: Forward TOF system LV power: 6.0KW (400 Amps). LV power feeds from platform: Custom two-conductor 12AWG tray rated cabling with embedded low voltage sense twisted pair wires.

Barrel TOF system LV power: 15.0KW (1,000 Amps). LV power feeds from platform: Custom two-conductor 8AWG or 10AWG (depending on LV segmentation) tray rated cabling with embedded low voltage sense twisted pair wires. Custom enclosed LV power distribution PCBs will be installed at the detector side and outside of the inner detector volume. A disconnect is required for each LV output port of the distribution box. Power distribution to the service hybrids will be configured to not exceed 10.0% channel segmentation from the rack-mount power control. Multi-channel ISEG ESH series power modules will provide up to negative 500VDC bias at a current of 10ma per channel. Multiconductor cables terminated with REDEL connectors or individual coax cables terminated with SHV connectors will feed an enclosed HV distribution box. The HV bias cabling to the detector hybrids will be carried over a multi-drop cable configuration to service the sensor hybrids in small groups.

**Schedule** Although there are still many uncertain elements at this stage, the latest schedule is shown in this section. The overall progress of development depends heavily on the advancement of the sensor. For instance, since the ASIC blueprint is based on the sensor's features, the ASIC design cannot be completed before the sensor development is finalized. This was the first principle we used to set up the schedule.

At least three sensor prototypes will be produced. The first prototype, the full-size sensor prototype, has already been manufactured by HPK. Based on the characteristics of this sensor, the FCFDv2 and EICROC2 ASICs will be developed. Based on our experience, we can also expect that the time required to fabricate the sensor and the ASIC will be 4 months from the submission of the design. Additionally, prototypes of the the Service Hybrid (SH), electronics (FPC for BTOF and module board for FTOF), and support structure will be created based on this sensor and ASIC.

Next, the design for the second full-size sensor prototype will incorporate improvements identified from the first prototype. The design will start 2 months later of starting the first sensor validation. The design of the next ASICs (FCFDv3 and EICROC3) will begin as soon as the sensor design is finalized. The SH, FPC, and stave support structure will also be developed in conjunction with this sensor and ASIC. Some characteristics of the sensor can be estimated based on accumulated knowledge, which might allow certain designs to be completed simultaneously.

The second full-size sensor prototype will be the last sensor prototype, but we will make another prototype as a backup and make final adjustments for mass production. Depending on the budget, additional sensor and ASIC prototypes may be ordered.

In the preproduction phase, 10% of the required number of prototypes are made in six months, during which time the final confirmation for mass production is made. Then, during the Production phase, the remaining 90% will be done in two years.

During the development phase, assembly was carried out as soon as the other components became available. However, in the preproduction and production phases, there will be a time lag between the arrival of components and the start of assembly. This is because additional time is required for quality assurance (QA) and quality control (QC) procedures before the components can be shipped to the dedicated assembly sites. As a result, the preproduction and production phases will begin two months later than other phases.

**particle identification** Figure 8.19 shows an example of a single-particle response simulation of $1/\beta$ as a function of particle momentum for BTOF and FTOF performance.

#### 8.3.4.2 The proximity focusing RICH

**Requirements**

**Requirements from physics:** Add text here.

**Requirements from Radiation Hardness:** Add text here.

**Requirements from Data Rates:** Add text here.

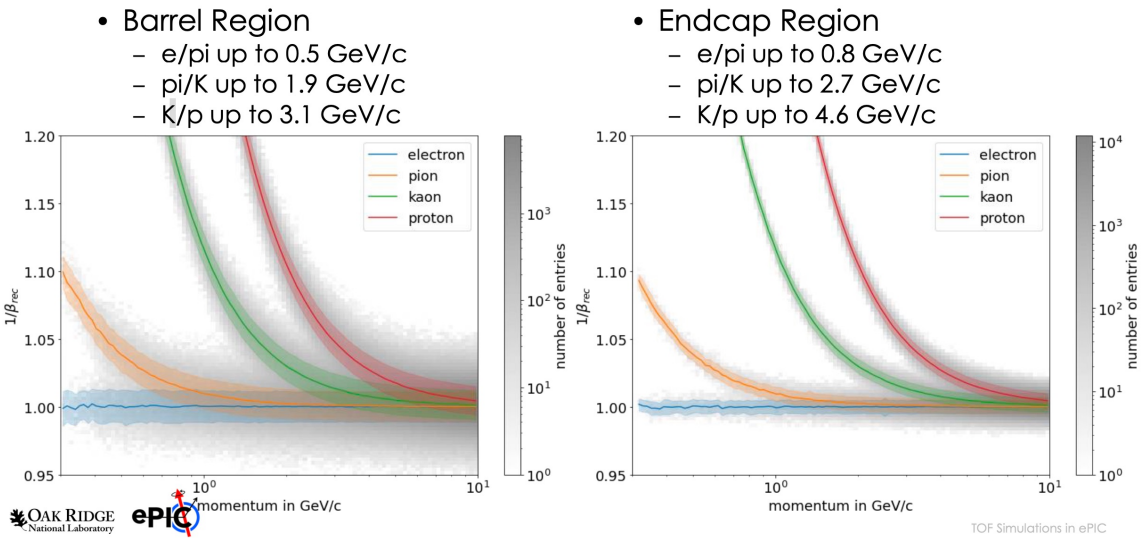


**Figure 8.19:** simulation of $1/\beta$ as a function of particle momentum for BTOF and FTOF performance.

### Justification

**Device concept and technological choice:** Add text here.

### Subsystem description:

General device description: Add text here.

Sensors: Add text here.

FEE: Add text here.

Other components: Add text here.

### Performance

### Implementation

**Services:** Add text here.

**Subsystem mechanics and integration:** Add text here.

**Calibration, alignment and monitoring:** Add text here.

**Status and remaining design effort:**

R&D effort: Add text here.

E&D status and outlook: Add text here.

Other activity needed for the design completion: Add text here.

Status of maturity of the subsystem: Add text here.

**Environmental, Safety and Health (ES&H) aspects and Quality Assessment (QA planning:** Add text here.

**Construction and assembly planning:** Add text here.

**Collaborators and their role, resources and workforce:** Add text here.

**Risks and mitigation strategy:** Add text here.

**Additional Material** Add text here.

#### 8.3.4.3 The high performance DIRC

**Requirements**

**Requirements from physics:** Add text here.

**Requirements from Radiation Hardness:** Add text here.

**Requirements from Data Rates:** Add text here.

**Justification**

**Device concept and technological choice:** Add text here.

**Subsystem description:**

General device description: Add text here.

Sensors: Add text here.

FEE: Add text here.

Other components: Add text here.

**Performance**

**Implementation**

**Services:** Add text here.

**Subsystem mechanics and integration:** Add text here.

**Calibration, alignment and monitoring:** Add text here.

**Status and remaining design effort:**

R&D effort: Add text here.

E&D status and outlook: Add text here.

Other activity needed for the design completion: Add text here.

Status of maturity of the subsystem: Add text here.

**Environmental, Safety and Health (ES&H) aspects and Quality Assessment (QA planning:** Add text here.

**Construction and assembly planning:** Add text here.

**Collaborators and their role, resources and workforce:** Add text here.

**Risks and mitigation strategy:** Add text here.

**Additional Material** Add text here.

#### 8.3.4.4 The dual radiator RICH

**Requirements**

**Requirements from physics:** Add text here.

**Requirements from Radiation Hardness:** Add text here.

**Requirements from Data Rates:** Add text here.

**Justification**

**Device concept and technological choice:** Add text here.

**Subsystem description:**

General device description: Add text here.

Sensors: Add text here.

FEE: Add text here.

Other components: Add text here.

**Performance**

**Implementation**

**Services:** Add text here.

**Subsystem mechanics and integration:** Add text here.

**Calibration, alignment and monitoring:** Add text here.

**Status and remaining design effort:**

R&D effort: Add text here.

E&D status and outlook: Add text here.

Other activity needed for the design completion: Add text here.

Status of maturity of the subsystem: Add text here.

**Environmental, Safety and Health (ES&H) aspects and Quality Assessment (QA planning:** Add text here.

**Construction and assembly planning:** Add text here.

**Collaborators and their role, resources and workforce:** Add text here.

**Risks and mitigation strategy:** Add text here.

**Additional Material** Add text here.

### 8.3.5 Electromagnetic Calorimetry

Add text here.

#### 8.3.5.1 The backward endcap electromagnetic calorimeter

**Requirements**

**Requirements from physics:** Add text here.

**Requirements from Radiation Hardness:** Add text here.

**Requirements from Data Rates:** Add text here.

**Justification**

**Device concept and technological choice:** Add text here.

**Subsystem description:**

General device description: Add text here.

Sensors: Add text here.

FEE: Add text here.

Other components: Add text here.

**Performance**

**Implementation**

**Services:** Add text here.

**Subsystem mechanics and integration:** Add text here.

**Calibration, alignment and monitoring:** Add text here.

**Status and remaining design effort:**

R&D effort: Add text here.

E&D status and outlook: Add text here.

Other activity needed for the design completion: Add text here.

Status of maturity of the subsystem: Add text here.

**Environmental, Safety and Health (ES&H) aspects and Quality Assessment (QA planning:** Add text here.

**Construction and assembly planning:** Add text here.

**Collaborators and their role, resources and workforce:** Add text here.

**Risks and mitigation strategy:** Add text here.

**Additional Material** Add text here.

#### 8.3.5.2 The barrel electromagnetic calorimeter

**Requirements**

**Requirements from physics:** Add text here.

**Requirements from Radiation Hardness:** Add text here.

**Requirements from Data Rates:** Add text here.

**Justification**

**Device concept and technological choice:** Add text here.

**Subsystem description:**

General device description: Add text here.

Sensors: Add text here.

FEE: Add text here.

Other components: Add text here.

**Performance**

**Implementation**

**Services:** Add text here.

**Subsystem mechanics and integration:** Add text here.

**Calibration, alignment and monitoring:** Add text here.

**Status and remaining design effort:**

R&D effort: Add text here.

E&D status and outlook: Add text here.

Other activity needed for the design completion: Add text here.

Status of maturity of the subsystem: Add text here.

**Environmental, Safety and Health (ES&H) aspects and Quality Assessment (QA planning:** Add text here.

**Construction and assembly planning:** Add text here.

**Collaborators and their role, resources and workforce:** Add text here.

**Risks and mitigation strategy:** Add text here.

**Additional Material** Add text here.

#### 8.3.5.3 The forward endcap electromagnetic calorimeter

**Requirements**

**Requirements from physics:** Add text here.

**Requirements from Radiation Hardness:** Add text here.

**Requirements from Data Rates:** Add text here.

**Justification**

**Device concept and technological choice:** Add text here.

**Subsystem description:**

General device description: Add text here.

Sensors: Add text here.

FEE: Add text here.

Other components: Add text here.

**Performance**

**Implementation**

**Services:** Add text here.

**Subsystem mechanics and integration:** Add text here.

**Calibration, alignment and monitoring:** Add text here.

**Status and remaining design effort:**

R&D effort: Add text here.

E&D status and outlook: Add text here.

Other activity needed for the design completion: Add text here.

Status of maturity of the subsystem: Add text here.

**Environmental, Safety and Health (ES&H) aspects and Quality Assessment (QA planning:** Add text here.

**Construction and assembly planning:** Add text here.

**Collaborators and their role, resources and workforce:** Add text here.

**Risks and mitigation strategy:** Add text here.

**Additional Material** Add text here.

### 8.3.6 Hadronic Calorimetry

Add text here.

#### 8.3.6.1 The backward endcap hadronic calorimeter

**Requirements**

**Requirements from physics:** Add text here.

**Requirements from Radiation Hardness:** Add text here.

**Requirements from Data Rates:** Add text here.

**Justification**

**Device concept and technological choice:** Add text here.

**Subsystem description:**

General device description: Add text here.

Sensors: Add text here.

FEE: Add text here.

Other components: Add text here.

**Performance**

**Implementation**

**Services:** Add text here.

**Subsystem mechanics and integration:** Add text here.

**Calibration, alignment and monitoring:** Add text here.

**Status and remaining design effort:**

R&D effort: Add text here.

E&D status and outlook: Add text here.

Other activity needed for the design completion: Add text here.

Status of maturity of the subsystem: Add text here.

**Environmental, Safety and Health (ES&H) aspects and Quality Assessment (QA planning:** Add text here.

**Construction and assembly planning:** Add text here.

**Collaborators and their role, resources and workforce:** Add text here.

**Risks and mitigation strategy:** Add text here.

**Additional Material** Add text here.

#### 8.3.6.2 The barrel hadronic calorimeter

**Requirements**

**Requirements from physics:** Add text here.

**Requirements from Radiation Hardness:** Add text here.

**Requirements from Data Rates:** Add text here.

**Justification**

**Device concept and technological choice:** Add text here.

**Subsystem description:**

General device description: Add text here.

Sensors: Add text here.

FEE: Add text here.

Other components: Add text here.

**Performance**

**Implementation**

**Services:** Add text here.

**Subsystem mechanics and integration:** Add text here.

**Calibration, alignment and monitoring:** Add text here.

**Status and remaining design effort:**

R&D effort: Add text here.

E&D status and outlook: Add text here.

Other activity needed for the design completion: Add text here.

Status of maturity of the subsystem: Add text here.

**Environmental, Safety and Health (ES&H) aspects and Quality Assessment (QA planning:** Add text here.

**Construction and assembly planning:** Add text here.

**Collaborators and their role, resources and workforce:** Add text here.

**Risks and mitigation strategy:** Add text here.

**Additional Material** Add text here.

#### 8.3.6.3 The forward endcap hadronic calorimeter

**Requirements**

**Requirements from physics:** Add text here.

**Requirements from Radiation Hardness:** Add text here.

**Requirements from Data Rates:** Add text here.

**Justification**

**Device concept and technological choice:** Add text here.

**Subsystem description:**

General device description: Add text here.

Sensors: Add text here.

FEE: Add text here.

Other components: Add text here.

**Performance**

**Implementation**

**Services:** Add text here.

**Subsystem mechanics and integration:** Add text here.

**Calibration, alignment and monitoring:** Add text here.

**Status and remaining design effort:**

R&D effort: Add text here.

E&D status and outlook: Add text here.

Other activity needed for the design completion: Add text here.

Status of maturity of the subsystem: Add text here.

**Environmental, Safety and Health (ES&H) aspects and Quality Assessment (QA planning:** Add text here.

**Construction and assembly planning:** Add text here.

**Collaborators and their role, resources and workforce:** Add text here.

**Risks and mitigation strategy:** Add text here.

**Additional Material** Add text here.

### 8.3.7 Far forward detectors

Add text here.

#### 8.3.7.1 The detectors in the B0 bending magnet

**Requirements**

**Requirements from physics:** Add text here.

**Requirements from Radiation Hardness:** Add text here.

**Requirements from Data Rates:** Add text here.

**Justification**

**Device concept and technological choice:** Add text here.

**Subsystem description:**

General device description: Add text here.

Sensors: Add text here.

FEE: Add text here.

Other components: Add text here.

**Performance**

**Implementation**

**Services:** Add text here.

**Subsystem mechanics and integration:** Add text here.

**Calibration, alignment and monitoring:** Add text here.

**Status and remaining design effort:**

R&D effort: Add text here.

E&D status and outlook: Add text here.

Other activity needed for the design completion: Add text here.

Status of maturity of the subsystem: Add text here.

**Environmental, Safety and Health (ES&H) aspects and Quality Assessment (QA planning:** Add text here.

**Construction and assembly planning:** Add text here.

**Collaborators and their role, resources and workforce:** Add text here.

**Risks and mitigation strategy:** Add text here.

**Additional Material** Add text here.

#### 8.3.7.2 The roman pots and the off-momentum detectors

**Requirements**

**Requirements from physics:** The Roman pots and Off-Momentum Detectors need to cover an angular region from $\sim$0 to 5 mrad. For the Roman pots, achieving acceptance down to 0 mrad is impossible due to the presence of the hadron beam itself, so the low-$\theta$ (low-$p_T$) acceptance is essentially entirely driven by the focusing quadrupoles (machine optics) before and after the interaction point. For IP-6, the choice of low-$\beta^*$ optics to maximize luminosity means the $10\sigma$ transverse size of the beam at the Roman pots location is larger, worsening the acceptance at the expense of high luminosity. Conversely, a choice can be made to reduce luminosity to improve low-$\theta$ acceptance at the Roman pots location. Given this set of operational parameters for the machine itself, it is required that the sensor packages have minimal dead area at the edges to take maximum advantage of the machine optics during data taking runs.

For resolution, the detectors must deliver $p_T$-resolution better than 10%.

**Requirements from Radiation Hardness:** Maximal radiation doses are shown to be ¡ $10^{12}$ 1 MeV neutron equivalaent for NIEL radiation, while ionizing doses are around 1 krad for the Roman pots region of ePIC.

**Requirements from Data Rates:** Rates during normal operations, with expected vacuum of $10^{-9}$ mbar, are a few Hz/channel.

**Justification**

**Device concept and technological choice:** Add text here.

**Subsystem description:**

General device description: The Roman pots and off-momentum detectors are both vacuum-based silicon sensors arranged into two stations for fully reconstructing protons at various magnetic rigidities, where rigidity here refers to the fraction of the momentum the proton has with respect to the steering dipoles design orbit momentum.

Sensors: AC-coupled low-gain avalanche diodes (AC-LGADs) are the technology of choice for these two subsystems due to their capabiltity to provide both high-precisions space and time information.

FEE: Add text here.

Other components: Add text here.

**Performance**

**Implementation**

**Services:** Add text here.

**Subsystem mechanics and integration:** Add text here.

**Calibration, alignment and monitoring:** Add text here.

**Status and remaining design effort:**

R&D effort: Add text here.

E&D status and outlook: Add text here.

Other activity needed for the design completion: Add text here.

Status of maturity of the subsystem: Add text here.

**Environmental, Safety and Health (ES&H) aspects and Quality Assessment (QA planning:** Add text here.

**Construction and assembly planning:** Add text here.

**Collaborators and their role, resources and workforce:** Add text here.

**Risks and mitigation strategy:** Add text here.

**Additional Material** Add text here.

#### 8.3.7.3 The zero degree calorimeter

**Requirements**

**Requirements from physics:** Add text here.

**Requirements from Radiation Hardness:** Add text here.

**Requirements from Data Rates:** Add text here.

**Justification**

**Device concept and technological choice:** Add text here.

**Subsystem description:**

General device description: Add text here.
Sensors: Add text here.
FEE: Add text here.
Other components: Add text here.

**Performance**

**Implementation**

**Services:** Add text here.

**Subsystem mechanics and integration:** Add text here.

**Calibration, alignment and monitoring:** Add text here.

**Status and remaining design effort:**

R&D effort: Add text here.

E&D status and outlook: Add text here.

Other activity needed for the design completion: Add text here.

Status of maturity of the subsystem: Add text here.

**Environmental, Safety and Health (ES&H) aspects and Quality Assessment (QA planning:** Add text here.

**Construction and assembly planning:** Add text here.

**Collaborators and their role, resources and workforce:** Add text here.

**Risks and mitigation strategy:** Add text here.

**Additional Material** Add text here.

### 8.3.8 Far backward detectors

Add text here.

#### 8.3.8.1 The luminosity system

**Requirements**

**Requirements from physics:** Add text here.

**Requirements from Radiation Hardness:** Add text here.

**Requirements from Data Rates:** Add text here.

**Justification**

**Device concept and technological choice:** Add text here.

**Subsystem description:**

General device description: Add text here.

Sensors: Add text here.

FEE: Add text here.

Other components: Add text here.

**Performance**

**Implementation**

**Services:** Add text here.

**Subsystem mechanics and integration:** Add text here.

**Calibration, alignment and monitoring:** Add text here.

**Status and remaining design effort:**

R&D effort: Add text here.

E&D status and outlook: Add text here.

Other activity needed for the design completion: Add text here.

Status of maturity of the subsystem: Add text here.

**Environmental, Safety and Health (ES&H) aspects and Quality Assessment (QA planning:** Add text here.

**Construction and assembly planning:** Add text here.

**Collaborators and their role, resources and workforce:** Add text here.

**Risks and mitigation strategy:** Add text here.

**Additional Material** Add text here.

#### 8.3.8.2 The low $Q^2$ taggers

**Requirements**

**Requirements from physics:** Add text here.

**Requirements from Radiation Hardness:** Add text here.

**Requirements from Data Rates:** Add text here.

**Justification**

**Device concept and technological choice:** Add text here.

**Subsystem description:**

General device description: Add text here.

Sensors: Add text here.

FEE: Add text here.

Other components: Add text here.

**Performance**

**Implementation**

**Services:** Add text here.

**Subsystem mechanics and integration:** Add text here.

**Calibration, alignment and monitoring:** Add text here.

**Status and remaining design effort:**

R&D effort: Add text here.

E&D status and outlook: Add text here.

Other activity needed for the design completion: Add text here.

Status of maturity of the subsystem: Add text here.

**Environmental, Safety and Health (ES&H) aspects and Quality Assessment (QA planning:** Add text here.

**Construction and assembly planning:** Add text here.

**Collaborators and their role, resources and workforce:** Add text here.

**Risks and mitigation strategy:** Add text here.

**Additional Material** Add text here.

### 8.3.9 Polarimeters

Add text here.

#### 8.3.9.1 The electron polarimeters

**Requirements**

**Requirements from physics:** Add text here.

**Requirements from Radiation Hardness:** Add text here.

**Requirements from Data Rates:** Add text here.

**Justification**

**Device concept and technological choice:** Add text here.

**Subsystem description:**

General device description: Add text here.
Sensors: Add text here.
FEE: Add text here.
Other components: Add text here.

**Performance**

**Implementation**

**Services:** Add text here.

**Subsystem mechanics and integration:** Add text here.

**Calibration, alignment and monitoring:** Add text here.

**Status and remaining design effort:**

R&D effort: Add text here.

E&D status and outlook: Add text here.

Other activity needed for the design completion: Add text here.

Status of maturity of the subsystem: Add text here.

**Environmental, Safety and Health (ES&H) aspects and Quality Assessment (QA planning:** Add text here.

**Construction and assembly planning:** Add text here.

**Collaborators and their role, resources and workforce:** Add text here.

**Risks and mitigation strategy:** Add text here.

**Additional Material** Add text here.

#### 8.3.9.2 The proton polarimeters

**Requirements**

**Requirements from physics:** Add text here.

**Requirements from Radiation Hardness:** Add text here.

**Requirements from Data Rates:** Add text here.

**Justification**

**Device concept and technological choice:** Add text here.

**Subsystem description:**

General device description: Add text here.

Sensors: Add text here.

FEE: Add text here.

Other components: Add text here.

**Performance**

**Implementation**

**Services:** Add text here.

**Subsystem mechanics and integration:** Add text here.

**Calibration, alignment and monitoring:** Add text here.

**Status and remaining design effort:**

R&D effort: Add text here.

E&D status and outlook: Add text here.

Other activity needed for the design completion: Add text here.

Status of maturity of the subsystem: Add text here.

**Environmental, Safety and Health (ES&H) aspects and Quality Assessment (QA planning:** Add text here.

**Construction and assembly planning:** Add text here.

**Collaborators and their role, resources and workforce:** Add text here.

**Risks and mitigation strategy:** Add text here.

**Additional Material** Add text here.

### 8.3.10 Readout Electronics and Data Acquisition

**Requirements**

**Requirements from physics:** Add text here.

**Requirements from Radiation Hardness:** Add text here.

**Requirements from Data Rates:** Add text here.

**Justification**

**Device concept and technological choice:** Add text here.

**Subsystem description:**

General device description: Add text here.

Sensors: Add text here.

FEE: Add text here.

Other components: Add text here.

**Performance**

**Implementation**

**Services:** Add text here.

**Subsystem mechanics and integration:** Add text here.

**Calibration, alignment and monitoring:** Add text here.

**Status and remaining design effort:**

R&D effort: Add text here.

E&D status and outlook: Add text here.

Other activity needed for the design completion: Add text here.

Status of maturity of the subsystem: Add text here.

**Environmental, Safety and Health (ES&H) aspects and Quality Assessment (QA planning:** Add text here.

**Construction and assembly planning:** Add text here.

**Collaborators and their role, resources and workforce:** Add text here.

**Risks and mitigation strategy:** Add text here.

**Additional Material** Add text here.

### 8.3.11 Software and Computing

**Requirements**

**Requirements from physics:** Add text here.

**Requirements from Radiation Hardness:** Add text here.

**Requirements from Data Rates:** Add text here.

**Justification**

**Device concept and technological choice:** Add text here.

**Subsystem description:**

General device description: Add text here.

Sensors: Add text here.

FEE: Add text here.

Other components: Add text here.

**Performance**

**Implementation**

**Services:** Add text here.

**Subsystem mechanics and integration:** Add text here.

**Calibration, alignment and monitoring:** Add text here.

**Status and remaining design effort:**

R&D effort: Add text here.

E&D status and outlook: Add text here.

Other activity needed for the design completion: Add text here.

Status of maturity of the subsystem: Add text here.

**Environmental, Safety and Health (ES&H) aspects and Quality Assessment (QA planning:** Add text here.

**Construction and assembly planning:** Add text here.

**Collaborators and their role, resources and workforce:** Add text here.

**Risks and mitigation strategy:** Add text here.

**Additional Material** Add text here.

## 8.4 Detector Integration

Add text here.

### 8.4.1 Installation and Maintenance

Add text here.

## 8.5 Detector Commissioning and Pre-Operations

Add text here.

# References


[1] R. Abdul Khalek et al. "Science Requirements and Detector Concepts for the Electron-Ion Collider: EIC Yellow Report". In: *Nucl. Phys. A* 1026 (2022), p. 122447. DOI: 10.1016/j.nuclphysa.2022.122447. arXiv: 2103.05419 [physics.ins-det].

[2] *Technical Design Report: A High-Granularity Timing Detector for the ATLAS Phase-II Upgrade*. Tech. rep. Geneva: CERN, 2020. URL: https://cds.cern.ch/record/2719855.

[3] C. Madrid et al. "First survey of centimeter-scale AC-LGAD strip sensors with a 120 GeV proton beam". In: *Journal of Instrumentation* 18.06 (June 2023), P06013. ISSN: 1748-0221. DOI: 10.1088/1748-0221/18/06/p06013. URL: http://dx.doi.org/10.1088/1748-0221/18/06/P06013.

[4] Irene Dutta and Christopher Madrid and Ryan Heller and Shirsendu Nanda and Danush Shekar and Claudio San Martín and Matías Barría and Artur Apresyan and Zhenyu Ye and William K. Brooks and Wei Chen and Gabriele D'Amen and Gabriele Giacomini and Alessandro Tricoli and Aram Hayrapetyan and Hakseong Lee and Ohannes Kamer Köseyan and Sergey Los and Koji Nakamura and Sayuka Kita and Tomoka Imamura and Cristían Peña and Si Xie. "Results for pixel and strip centimeter-scale AC-LGAD sensors with a 120 GeV proton beam". In: (July 2024). arXiv: 2407.09928 [physics.ins-det].

[5] C. Bishop et al. "Long-distance signal propagation in AC-LGAD". In: *Nuclear Instruments and Methods in Physics Research Section A: Accelerators, Spectrometers, Detectors and Associated Equipment* 1064 (2024), p. 169478. ISSN: 0168-9002. DOI: https://doi.org/10.1016/j.nima.2024.169478. URL: https://www.sciencedirect.com/science/article/pii/S0168900224004042.

[6] L. Menzio et al. "First test beam measurement of the 4D resolution of an RSD pixel matrix connected to a FAST2 ASIC". In: *Nucl. Instrum. Meth. A* 1065 (2024), p. 169526. DOI: 10.1016/j.nima.2024.169526. arXiv: 2402.01517 [physics.ins-det].

[7] S. Xie et al. "Design and performance of the Fermilab Constant Fraction Discriminator ASIC". In: *Nuclear Instruments and Methods in Physics Research Section A: Accelerators, Spectrometers, Detectors and Associated Equipment* 1056 (2023), p. 168655. DOI: https://doi.org/10.1016/j.nima.2023.168655. URL: https://www.sciencedirect.com/science/article/pii/S0168900223006459.

[8] C. Chock et al. “First test results of the trans-impedance amplifier stage of the ultra-fast HPSoC ASIC”. In: *Journal of Instrumentation* 18.02 (2023), p. C02016. DOI: 10.1088/1748-0221/18/02/C02016. URL: https://dx.doi.org/10.1088/1748-0221/18/02/C02016.